

# **Vehicle-to-Grid Technology Employing DC Fast Charging Configuration in a Microgrid Using Fuzzy Logic Controller**

**SESHASAI BAGADI (Research Scholar)<sup>1</sup>**, SRI VENKATESWARA COLLEGE OF ENGINEERING & TECHNOLOGY NH-5, Etcherla, SRIKAKULAM (A.P)-532410  
**A. APPARAO , M.Tech (Ph.D.)(Associate Professor & HOD)<sup>2</sup>**, SRI VENKATESWARA COLLEGE OF ENGINEERING & TECHNOLOGY NH-5, Etcherla, SRIKAKULAM (A.P)-532410  
**VENKATESWARA RAO K, M. Tech, (Ph.D.)<sup>3</sup>**, GOVERNMENT POLYTECHNIC PARVATHIPURAM, VIZIANAGARAM (Dist) (A.P)-535501

**Abstract:** In micro-grids, electric vehicle (EV) batteries could be used as energy storage devices. They can assist with micro-grid energy management by storing energy when there is a surplus (Grid-To-Vehicle, G2V) and supplying energy back to the grid when there is a demand for it (Vehicle-To-Grid, V2G). To make this vision a reality, the necessary infrastructure and control mechanisms must be created. This study presents architecture for establishing a V2G-G2V system in a micro-grid with level-3 fast charging of EVs. A micro-grid test system with a dc rapid charging station for interfacing the electric vehicles is modeled. V2G-G2V power transfer is demonstrated through simulation research. The results of the tests reveal that EV batteries may actively regulate power in the microgrid using G2V-V2G modes of operation. The charging station's design provides that grid injected current has no more harmonic distortion, and the controller delivers high dynamic performance in terms of dc bus voltage stability.

**Index term:** DC fast charging, Electric vehicle, Grid connected inverter, Micro-grid, Off-board charger, Vehicle-to-grid

## **I. INTRODUCTION**

Energy storage systems are crucial components of a microgrid because they allow intermittent renewable energy sources to be integrated. When EV batteries are plugged in for charging, they can be used as storage devices in micro-grids. Most personal transportation cars are parked for around 22 hours every day, representing an idle asset. EVs could potentially aid micro-grid energy management by storing excess energy (Grid-To-Vehicle, G2V) and feeding it back to the grid when there is a demand for it (Vehicle-To-Grid). V2G in the general power grid confronts several challenges, such as being difficult to control, requiring a large number of EVs, and being difficult to implement quickly [1]. In this scenario, a V2G system in a micro-grid is easy to set up.

For electric vehicles, the Society of Automotive Engineers has three charging levels. The vehicle's on-board charger is connected to a socket that plugs into a typical household (120 V) outlet for Level 1 charging. This is the slowest charging method and is best for people who travel less than 60 kilometres per day and have all night to charge.

At home or at a public station, a dedicated Electric Vehicle Supply Equipment (EVSE) provides electricity at 220 V or 240 V and up to 30 A for level 2 charging. DC rapid charging is a term used to describe level 3 charging. DC fast charging stations can deliver up to 90 kW of charging power at 200/450 V, reducing charging time to 20-30 minutes.

Due to the rapid power transfer necessary when EVs are used for energy storage, DC fast charging is chosen for implementing V2G architecture in a microgrid. The dc bus can also be utilised to include renewable generation into the system. The dc bus can also be utilised to include renewable generation

into the system.

The V2G approach has been used in the general power grid for services such as peak shaving, valley filling, regulation, and spinning reserves in the majority of prior studies [2]. The development of V2G technology in a micro-grid facility to support power generation from intermittent renewable energy sources is still in its early stages. In addition, most of the works described [3] use level 1 and level 2 ac charging for V2G technology. These ac charging systems are limited by the on-board charger's power rating. Another problem is that the distribution infrastructure was not built to handle bi-directional energy flow. In this case, research is needed to design technically viable charging station architectures to enable V2G technology in micro-grids. In a micro-grid facility, this work presents a dc rapid charging station infrastructure with V2G functionality. A solar photovoltaic (PV) array is integrated into the micro-grid using the same dc bus that connects EVs. Off-board chargers can provide high-power bi-directional charging for EVs under the proposed architecture. The proposed model's effectiveness is assessed using MATLAB/Simulink simulations in both V2G and G2V modes of operation.

## II. CONFIGURATION OF A DC FAST CHARGING STATION FOR V2G

The Figure 1 [4] shows the configuration of a dc rapid charging station for implementing V2G-G2V infrastructure in a micro-grid. Off-board chargers connect electric vehicle batteries to the dc bus. Through an LCL filter and a step-up transformer, a grid linked inverter connects the dc bus to the utility grid. The charging station's essential important components are listed below.

### A. Battery Charger Configuration

The chargers for dc fast charging are placed off-board and housed in an EVSE. The essential building component of an off-board charger with V2G functionality is a bidirectional dc-dc converter. It connects the electric vehicle battery system to the dc distribution grid. Figure 2 depicts the converter arrangement. It consists of two IGBT/MOSFET switches controlled by complementary control signals at all moments.

1) **Buck mode of operation (charging mode):** The converter functions as a buck converter when the upper switch ( $S_{buck}$ ) is activated, stepping down the input voltage ( $V_{dc}$ ) to the battery charging voltage ( $V_{batt}$ ). Current travels through the switch and inductor to the battery when the switch is turned on. This is the charging process, in which power is transferred from the grid to the vehicle (G2V).

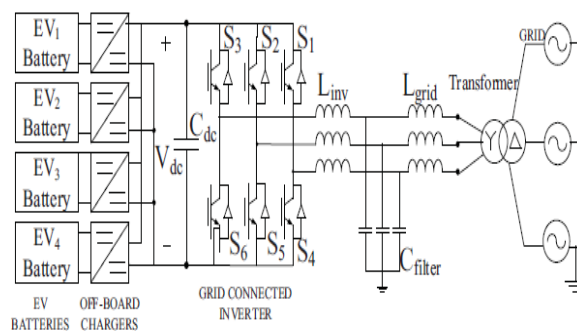


Fig. 1. EV charging station for fast dc charging

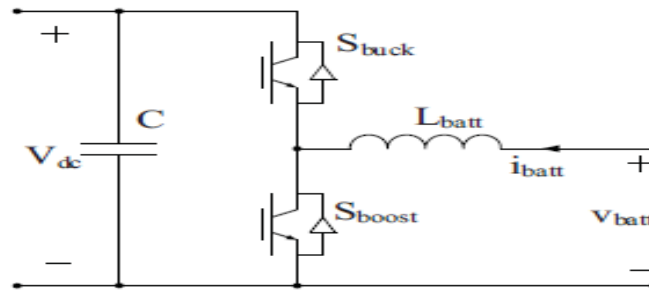


Fig. 2. Battery charger configuration

When the switch is turned off, the current flows back through the lower switch's inductor and diode, completing the circuit. If  $D$  is the upper switch's duty ratio, the battery voltage is calculated as follows:

$$V_{batt} = V_{dc} * D \quad (1)$$

2) Boost mode of operation (discharging mode): The converter operates as a boost converter when the lower switch is turned on, stepping up the battery voltage to the dc bus voltage. When the switch is in the on position, current continues to flow through the inductor and completes the circuit via the upper switch's anti-parallel diode and the capacitor. In this situation, the battery is in the discharge state and the net power flow is from the vehicle to the grid (V2G). If the capacitor is large enough to provide a constant dc voltage, the output voltage during boost mode of operation is given by:

$$V_{dc} = \frac{V_{batt}}{1 - D'} \quad (2)$$

Where  $D'$  is the duty cycle of the lower switch.

## B. Grid Connected Inverter and LCL Filter

The grid connected inverter (GCI) converts dc bus voltage to three-phase ac voltage and permits current to flow backwards through anti-parallel diodes in each leg's switches (Fig. 1). An LCL filter is connected to the inverter's output terminals to reduce harmonics and produce pure sinusoidal voltage and current. This work's design technique for calculating the LCL filter parameters is based on [4].

## CONTROL SYSTEM

### A. Off-Board Charger Control

For charge/discharge control of the battery charger circuit, a constant current control approach [5] using PI controllers is used, as shown in Fig.3. To determine the polarity of the current signal and choose between charging and discharging modes of operation, the controller compares the reference battery current to zero. After selecting the mode, the reference current is compared to the measured current, and the error is transferred via a PI controller to generate  $S_{buck}/ S_{boost}$  switching pulses. During the charging phase,  $S_{boost}$  will be turned off, and  $S_{buck}$  will be turned off during the discharging process.

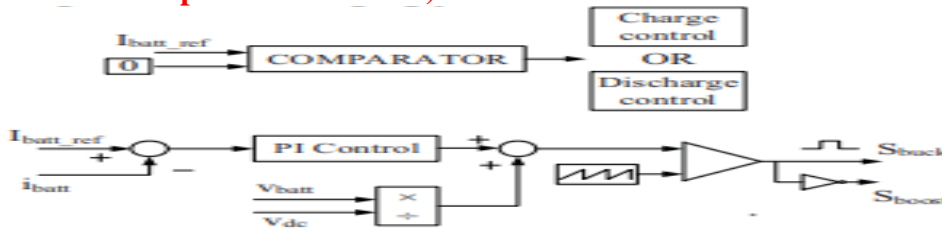


Fig. 3. Constant current control strategy for battery charger

B. Inverter Control

For the inverter controller, a cascade control in synchronous reference frame is presented. Two outside voltage control loops and two inner current control loops made up the control structure. The active ac current is controlled by the d-axis inner loop, while the dc bus voltage is controlled by the outer loop. Similarly, the q-axis outer loop regulates the reactive current, which is regulated by the q-axis inner current loop, to regulate the ac voltage magnitude. To boost performance during transients, dq decoupling terms  $\omega L$  and feed-forward voltage signals have been introduced.

I. MICRO-GRID TEST SYSTEM CONFIGURATION

The Figure 5 shows the configuration of the micro-grid test system with the dc rapid charging station. The system's generation sources include a 100 kW wind turbine (WT) and a 50 kW solar PV array.

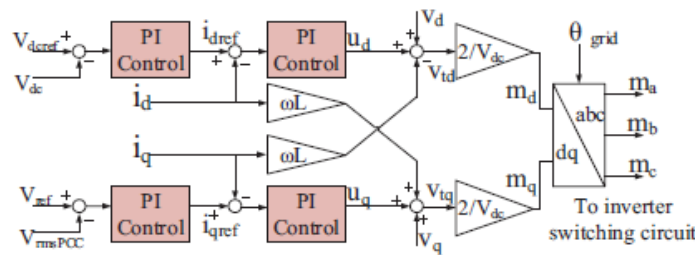


Fig. 4. Inverter control system

The EV battery storage system comprises of four EV batteries that are connected to the charging station's 1.5 kV dc bus through off-board chargers. A boost converter with a maximum power point tracking (MPPT) controller connects the solar PV to this dc bus as well. A 25 kV distribution feeder and a 120 kV equivalent transmission system contain the utility grid. At the point of common coupling, the wind turbine-driven doubly-fed induction generator is connected to the micro-grid (PCC). Transformers are used to increase voltages and connect the ac systems to the utility grid.

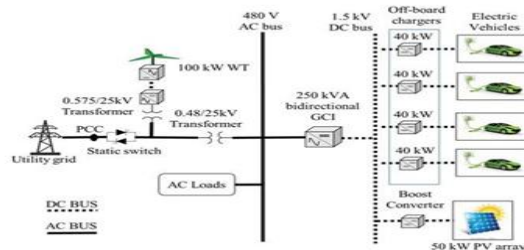


Fig 5. Proposed microgrid test system configuration

SIMULATION RESULTS

The process for designing charging stations was derived from [4], and the obtained parameter values are listed in Appendix. The wind turbine is set to its rated speed, producing a maximum output power of 100 kW. The solar PV system is tested under normal test circumstances (1000W/m<sup>2</sup> irradiance and 25°C temperature) and produces a maximum power output of 50 kW. The 480 V ac bus is connected to a 150 kW resistive load. For unity pf operation, the reactive current reference to GCI is set to zero. The initial state of charge (SOC) of the electric vehicle batteries is set to 50%. Once the steady state conditions have been achieved, the V2G-G2V power transfer is performed using the batteries of EV1 and EV2 (Fig. 1). Table I shows the current set-points for the battery charging circuits of the EV1 and EV2 batteries, with the results illustrated in the following figures. The Figs. 6 and 7 as shown the battery parameters when EV1 is operating in V2G mode and EV2 are operating in G2V mode, respectively.

**TABLE I. CURRENT SET-POINTS TO EV BATTERIES**

Time range (s)	0 to 1	1 to 4	4 to 6
Current set-point to EV <sub>1</sub> battery (A)	0	+80	0
Current set-point to EV <sub>2</sub> batter y(A)	0	0	-40

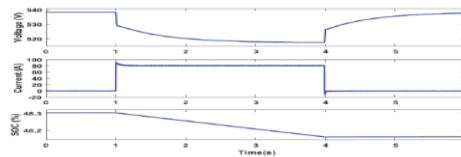


Fig. 6. Voltage, current, and SOC of EV<sub>1</sub> battery during V2G operation

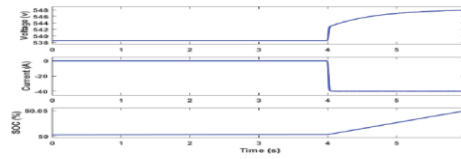


Fig. 7. Voltage, current, and SOC of EV<sub>2</sub> battery during G2V operation

The Figure 8 depicts the active power contribution from various system components. To accommodate the electricity transferred by the EVs, the grid power changes. The negative polarity of the grid power from 1s to 4s indicates that the vehicle is supplying power to the grid. At 4s, the polarity of grid power changes, indicating that the grid is supplying electricity to charge the vehicle battery. The V2G-G2V procedure is demonstrated in this example. Furthermore, the net power at PCC is zero, indicating that the system's power balance is appropriate.

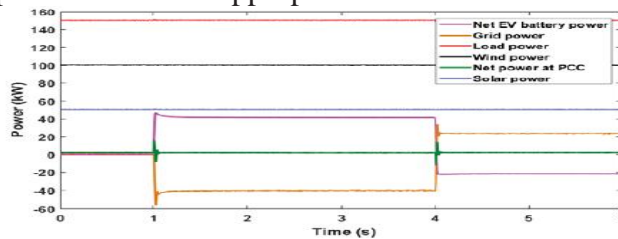


Fig. 8. Active power profile of various components in the system

The inverter controller's outer voltage control loop regulates the dc bus voltage at 1500 V, as shown in Fig. 9. The inner current control loop, as shown in Fig. 10, does this by tracking the changed d-axis reference current.

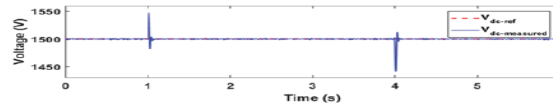


Fig. 9. Variation in dc bus voltage

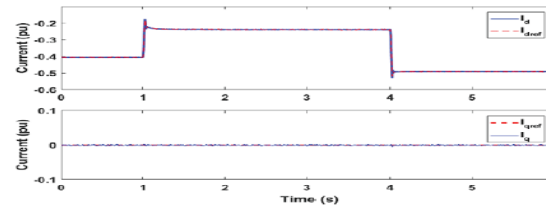


Fig. 10. Reference current tracking by inverter controller

Figure 11 depicts the grid voltage and current at PCC. During G2V operation, voltage and current are in phase, but during V2G operation, they are 180° out of phase, indicating reverse power flow.

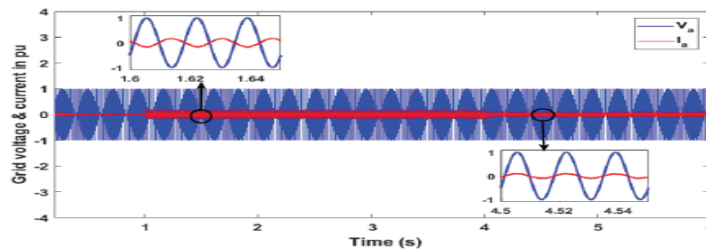


Fig. 11. Grid voltage and grid injected current during V2G-G2V operation

The grid injected current is subjected to a total harmonic distortion (THD) analysis, as shown in Fig. 12. Harmonic current distortion for power systems 69 kV and below is limited to 5% THD, according to IEEE Std. 1547. The THD of grid-injected current is 2.31 %, which is achieved through the careful design of the LCL filter.

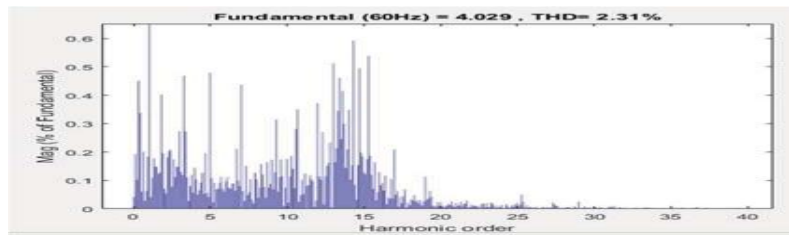


Fig.12. Harmonic spectrum and THD of grid-injected current

### **FUZZY LOGIC CONTROLLER:**

A set of linguistic principles governs basic control action in FLC. The system establishes these regulations. In FC, mathematical modeling of the system is not necessary because numerical variables are translated to linguistic variables. Fuzzification, interference engine, and defuzzification are the three sections of the FLC. The FC is defined as follows: i. each input and output has seven fuzzy sets. ii. For simplicity, triangular membership functions are used. iii. The use of a continuous universe of discourse for fuzzification. iv. Mamdani's "min" operator is used to infer. v. Using the "height" approach to defuzzify.

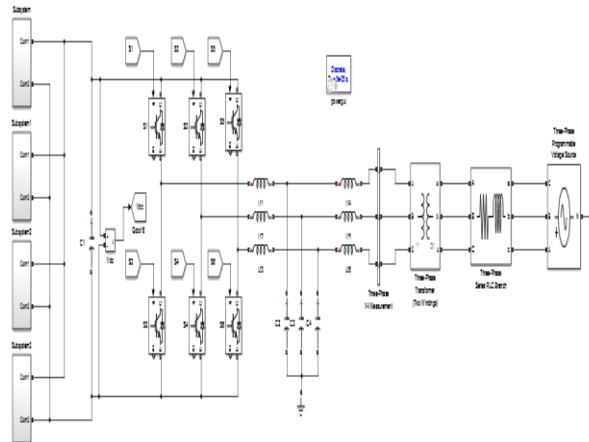
### **Fuzzification:**

Membership function values are assigned to the linguistic variables, using seven fuzzy subsets: NB (Negative Big), NM (Negative Medium), NS (Negative Small), ZE (Zero), PS (Positive Small), PM 5 (Positive Medium), and PB (Positive Big). The partition of fuzzy subsets and the shape of membership

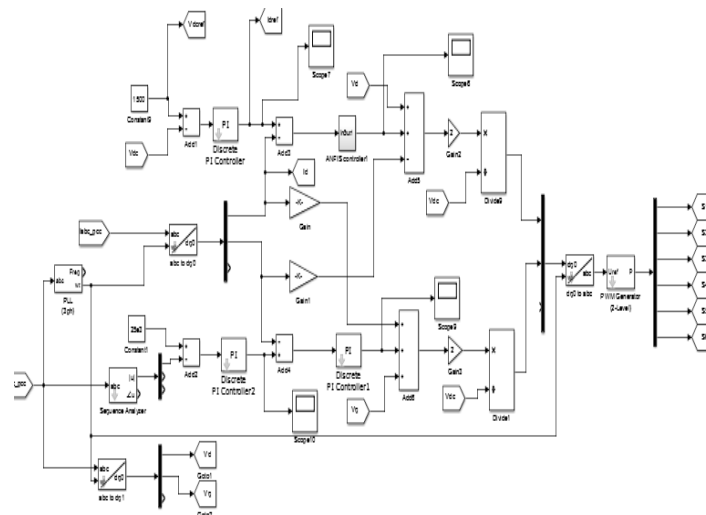
$CE(k)$   $E(k)$  function adapt the shape up to appropriate system. The value of input error and change in error are normalized by an input scaling factor.

$\Delta E$ \ $E$	NB	NM	NS	Z	PS	PM	PB
NB	NB	NB	NB	NB	NM	NS	Z
NM	NB	NB	NB	NM	NS	Z	PS
NS	NB	NB	NM	NS	Z	PS	PM
Z	NB	NM	NS	Z	PS	PM	PB
PS	NM	NS	Z	PS	PM	PB	PB
PM	NS	Z	PS	PM	PB	PB	PB
PB	Z	PS	PM	PB	PB	PB	PB

In this system the input scaling factor has been designed such that input values are between -1 and +1. The triangular shape of the membership function of this arrangement presumes that for any particular  $E(k)$  input there is only one dominant fuzzy subset.



Simulation diagram



Fuzzy logic controller of simulation diagram

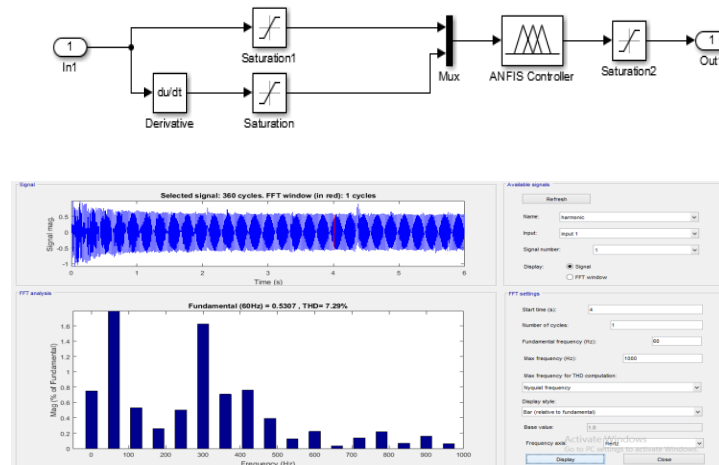


Fig.13. Harmonic spectrum and THD of grid-injected current using FLC

The results of Fuzzy logic controller optimization are compared to those of a traditional controller and PI controller, and better results are produced. The Fuzzy logic controller is performing dynamic response, reduced transient response and harmonic.

### CONCLUSIONS

This study presents the modeling and design of a V2G system in a micro-grid using a dc rapid charging architecture. To link EVs to the micro-grid, a dc rapid charging station with off-board chargers and a grid connected converter is designed. This power electronic interface's control mechanism permits bi-directional power transfer between EVs and the grid. The study further established a smooth power transfer between the EVs and the grid, with grid injected current from the EVs exceeding all applicable standards. In terms of dc bus voltage stability and tracking the changed active power reference, the developed controller performs well dynamically. This paper considers the microgrid's active power regulation features, and the proposed V2G system can be used for a variety of different services such as reactive power control and frequency regulation. Future research should focus on the design of a supervisory controller that sends command signals to the individual EV charging controllers. The Fuzzy logic controller is performing dynamic response, reduced transient response and harmonic.

### REFERENCES

- [1] C. Shumei, L. Xiaofei, T. Dewen, Z. Qianfan, and S. Liwei, "The construction and simulation of V2G system in micro-grid," in *Proceedings of the International Conference on Electrical Machines and Systems, ICEMS 2011*, 2011, pp. 1–4.
- [2] S. Han, S. Han, and K. Sezaki, "Development of an optimal vehicle-to-grid aggregator for frequency regulation," *IEEE Trans. Smart Grid*, vol. 1, no. 1, pp. 65–72, 2010.
- [3] M. C. Kisacikoglu, M. Kesler, and L. M. Tolbert, "Single-phase on-board bidirectional PEV charger for V2G reactive power operation," *IEEE Trans. Smart Grid*, vol. 6, no. 2, pp. 767–775, 2015.
- [4] A. Arancibia and K. Strunz, "Modeling of an electric vehicle charging station for fast DC charging," in *Proceedings of the IEEE International Electric Vehicle Conference (IEVC)*, 2012, pp. 1–6.
- [5] K. M. Tan, V. K. Ramachandaramurthy, and J. Y. Yong, "Bidirectional battery charger for electric vehicle," in *2014 IEEE Innovative Smart Grid Technologies - Asia, ISGT ASIA 2014*, 2014, pp. 406–411.



- [6] G.Chandrasekhar, M.Venkatesh and A.Appa Rao, “Wind Energy Source interfacing to Grid by using five level Inverter” in *2017 IJCTA International science press 10(5) 2017*, pp. 577–587

**APPENDIX**  
**CHARGING STATION PARAMETERS**

Parameter	Value	Parameter	Value
Rated capacity	250 kVA	EV rated power	40 kW
$V_{batt}$	500 V	Battery capacity	48 Ah
$C_{dc}$	850 $\mu$ F	$C_{filter}$	133 $\mu$ F
$L_{inv}$	0.25 mH	$L_{grid}$	0.25 mH